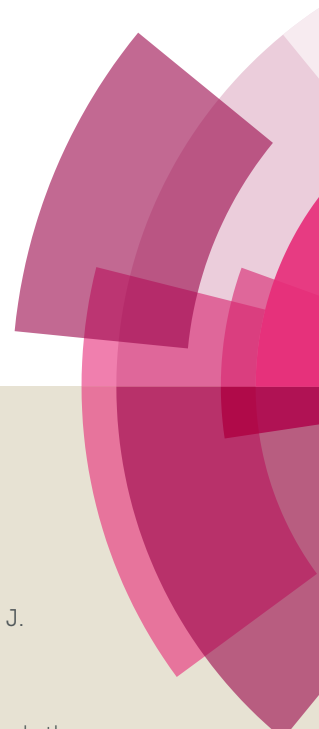


NJC

Accepted Manuscript



This article can be cited before page numbers have been issued, to do this please use: K. Jeyalakshmi, J. Haribabu, C. Balachandran, E. Narmatha, N. Bhuvanesh, S. Aoki and R. Karvembu, *New J. Chem.*, 2019, DOI: 10.1039/C8NJ04246B.



This is an Accepted Manuscript, which has been through the Royal Society of Chemistry peer review process and has been accepted for publication.

Accepted Manuscripts are published online shortly after acceptance, before technical editing, formatting and proof reading. Using this free service, authors can make their results available to the community, in citable form, before we publish the edited article. We will replace this Accepted Manuscript with the edited and formatted Advance Article as soon as it is available.

You can find more information about Accepted Manuscripts in the [author guidelines](#).

Please note that technical editing may introduce minor changes to the text and/or graphics, which may alter content. The journal's standard [Terms & Conditions](#) and the ethical guidelines, outlined in our [author and reviewer resource centre](#), still apply. In no event shall the Royal Society of Chemistry be held responsible for any errors or omissions in this Accepted Manuscript or any consequences arising from the use of any information it contains.

Highly Active Copper(I) Complexes of Aroylthiourea Ligands Against Cancer Cells – Synthetic and Biological Studies

Kumaramangalam Jeyalakshmi,^{a,b} Jebiti Haribabu,^a Chandrasekar Balachandran,^c Eswaramoorthi Narmatha,^a Nattamai S. P. Bhuvanesh,^d Shin Aoki,^c and Ramasamy Karvembu^{*a}

Abstract

The reaction of copper(I) bromide with aroylthiourea ligands (L) in the molar ratio 1:3, resulted in the formation of [CuBr(L)₃]. The complexes were well characterized by analytical and spectroscopic (UV-Visible, FT-IR, NMR and mass) techniques. Tetrahedral geometry of complexes **1** and **3** was confirmed by single crystal X-ray diffraction study. The interaction of complexes with biomolecules (DNA/protein) has been evaluated using spectrophotometric and spectrofluorometric techniques. The compounds were screened for its *in vitro* cytotoxicity against cancer and normal cell lines. Complexes **1** and **2** showed potent cytotoxic activity against HeLa cells with IC₅₀ value of 1.23 and 0.47 μM, respectively. The staining and colony formation studies were also carried out for the most active complexes to predict the morphological changes and colony formation ability respectively.

^aDepartment of Chemistry, National Institute of Technology, Tiruchirappalli 620015, India

^bDepartment of Chemistry, M. Kumarasamy College of Engineering, Karur 639113, India

^cFaculty of Pharmaceutical Sciences, Tokyo University of Science, 2641 Yamazaki, Noda 278-8510 Japan

^dDepartment of Chemistry, Texas A & M University, College Station, TX 77842, USA

Electronic supplementary information (ESI) available: Graphs of the binding experiments. Crystallographic data for the structures reported in this paper have been deposited with the Cambridge Crystallographic Data Centre (CCDC) as supplementary publication numbers CCDC 1850757-1850758. Copies of the data can be obtained free of charge from the CCDC (12 Union Road, Cambridge CB2 1EZ, UK; Tel.: + 44-1223-336408; Fax: +44-1223-336003; e-mail: deposit@ccdc.cam.ac.uk; web site: <http://www.ccdc.cam.ac.uk>).

1. Introduction

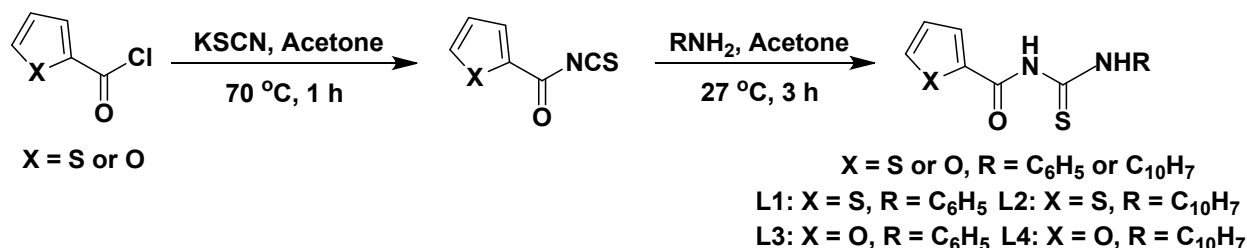
The research on the development of metal based drugs has attained a great significance after the discovery of cisplatin as an anticancer drug. Copper is an essential trace element in the biological systems, existing in the +2 and +1 oxidation states. It is employed as a structural and catalytic cofactor, and consequently involved in many biological pathways.¹⁻³ There are numerous reports on the biological applications of copper(II) complexes. In contrast to copper(II) complexes, reports on the biological applications of copper(I) complexes are scarce due to lower stability of the +1 oxidation state and their tendency towards oxidation to Cu(II) compounds. However, there are few reports which strongly evidenced the anticancer activity of copper(I) complexes. Copper(I) complexes bearing *tris*(hydroxymethyl)phosphine ligands inhibited the tumor growth *via* G2/M cell cycle arrest and paraptosis accompanied by the loss of mitochondrial transmembrane potential.⁴ Mixed ligand Cu(I) complexes of triazolylborate and alkyl- or aryl-phosphines have been found to be effective against A549 adenocarcinoma cells which are resistant to cisplatin.⁵ Binary Cu(I) complexes bearing 1,3,5-triaza-7-phosphaadamantane exhibited moderate cytotoxicity against various cancer cell lines.⁶

Copper(I) ion has a strong affinity to form bonds with ligands containing P or S donor atoms.⁷⁻¹² Such sulfur coordinated copper complexes acquire great importance due to its resemblance to the active centers of some copper proteins, hemocyanin and tyrosinase, which mediate redox and electron transfer reactions in biological systems. In this view, we have synthesized copper(I) complexes containing aroylthiourea ligands. Aroylthiourea is a versatile complexing agent capable of coordinating through O/S atom(s) by mono or bidentate fashion. Thiourea and its metal complexes found significant interest due to its wide range of biological activities such as antiviral, antibacterial, antifungal, antitubercular, antiinflammatory, anticancer, herbicidal and insecticidal.¹³⁻¹⁷ Our group has explored the biological activities of Cu(II), Ni(II), Pd(II) and Ru(II) complexes of aroylthiourea ligands.¹⁸⁻²⁴ In continuation of our interest in aroylthiourea complexes, we have synthesized the copper(I) complexes of aroylthiourea ligands. The binding propensity of synthesized complexes with DNA/protein was investigated. The compounds were also subjected to MTT assay to assess its cytotoxicity against various cancer and normal cell lines. Staining and colony formation assays were also carried out to support the cytotoxic ability of complexes.

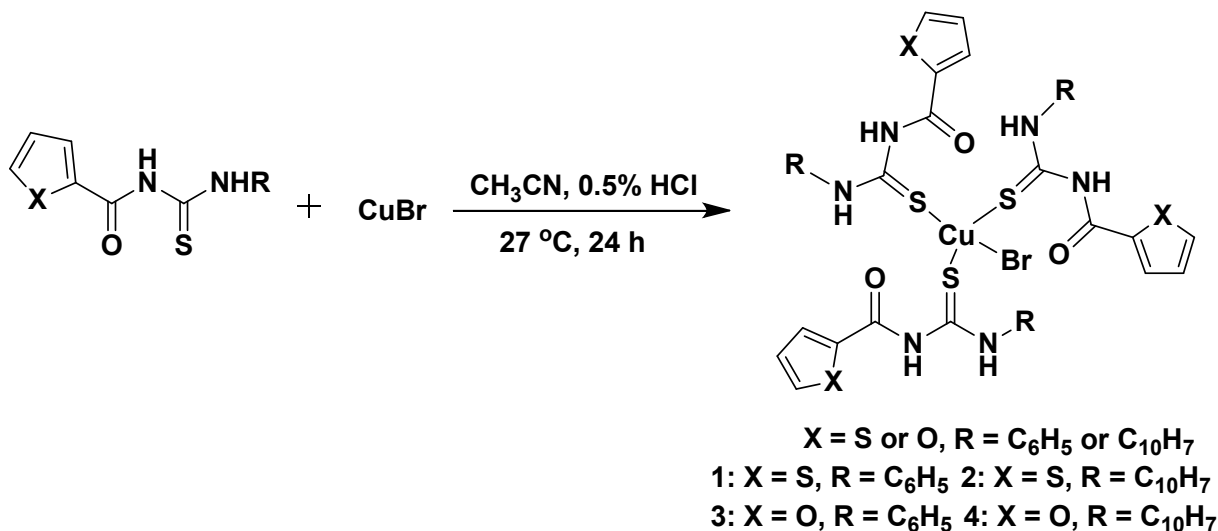
2. Results and discussion

2.1. Synthesis

The ligands were prepared from thiophene-2-carbonyl chloride/furoyl chloride, potassium thiocyanate and aniline/1-naphthyl amine (Scheme 1). The ligands on reaction with CuBr in acidic media (3:1 ratio) yielded complexes with the general formula [CuBr(L)₃] (Scheme 2). The ligands and their Cu(I) complexes were characterized by UV-Visible, FT-IR, NMR and single crystal X-ray diffraction techniques.



Scheme 1 Synthesis of the aroylthiourea ligands



Scheme 2 Synthesis of the copper(I) complexes

2.2. Spectroscopy

The UV-Visible spectra of ligands showed two bands around 261-263 and 283-296 nm, which corresponded to $\pi \rightarrow \pi^*$ and $n \rightarrow \pi^*$ transitions respectively. The spectra of complexes were similar to those of uncoordinated ligands with minor shift in the position of the peaks. There was no shift in the UV-Visible spectral bands of the complexes when it was recorded in DMF after 24

h. This confirms the stability of complexes in solution. The bands observed in the FT-IR spectra of ligands at 3121-3657, 1663-1669 and 1263-1275 cm^{-1} were assigned to $\nu(\text{N-H})$, $\nu(\text{C=O})$ and $\nu(\text{C=S})$ respectively. The decrease in the stretching frequency of C=S confirmed the coordination of sulphur to copper(I) ion.

^1H NMR spectra of L4 and complexes (**1-4**) are shown in figures S1-S5. In the ^1H NMR spectra of Cu(I) complexes, the carbonyl- and thiocarbonyl- attached N-H and thiocarbonyl- attached N-H protons were observed around 10.45-11.49 and 12.51-12.87 ppm, respectively. Signals due to protons of aromatic rings in **1-4** appeared at 7.78-8.19 ppm. The ^1H NMR spectra of ligand L2 and complex **2** are shown in figure 1. On complexation, there was a significant shift in the signal due to amide N-H proton. In the ^{13}C NMR spectra of complexes, the signals appeared around 113.2-149.0 ppm, which were due to the aromatic carbons (Figs. S6-S10). The resonances due to C=O and C=S carbons were observed around 162.8-163.6 and 178.3-180.8 ppm, respectively.²⁵

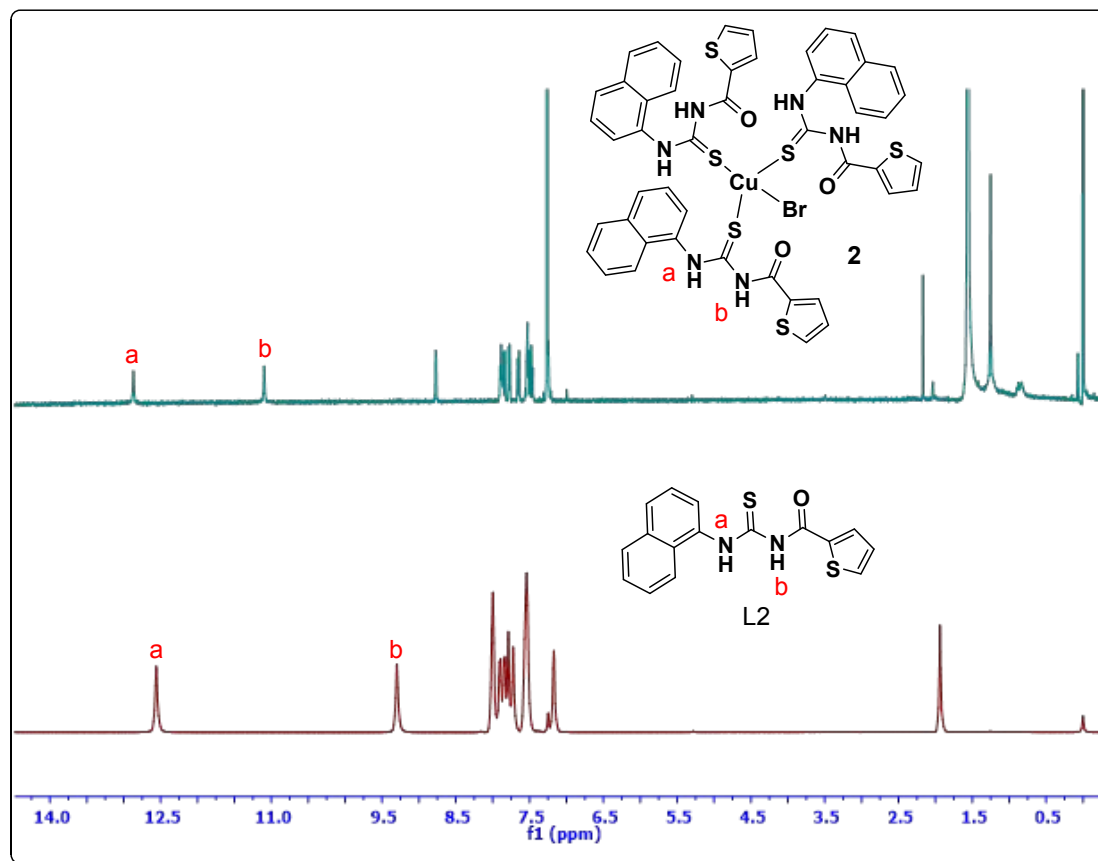


Fig. 1 ^1H NMR spectra of ligand L2 and complex **2**.

2.3. Structure

The molecular structures of complexes along with crystallographic numbering schemes are depicted in figures 2 and 3. Crystal data and selected inter atomic bond lengths and angles are tabulated (Tables 1 and 2). The crystals of complexes **1** and **3** were obtained from the slow evaporation of their chloroform/methanol solution. Complexes **1** and **3** crystallized in triclinic crystal system with space group *P*-1. The crystal structures confirmed tetrahedral geometry of copper(I) complexes where three coordination sites were occupied by sulphur from the aroylthiourea ligands and bromide occupied the fourth coordination site. The Cu–S bond distances were in the range of 2.2694–2.3034 Å and the average Cu–S distance was 2.2821 and 2.2804 Å for complexes **1** and **3** respectively. The S–Cu–S angles ranged from 108.15 to 111.37° in **1**, and 107.02 to 111.35° in **3**. The Br–Cu–S angles were in the range of 107.72–110.41° (**1**) and 107.04–112.21° (**3**), and their average value was close to that of ideal tetrahedral geometry. The crystal structures depicted the existence of intramolecular hydrogen bonding between NH and carbonyl O (N–H···O) in complexes **1** and **3**.^{23,26} In complex **3**, there was also an intramolecular hydrogen bonding between NH and coordinated Br ion (N–H···Br).

Table 1 Crystal data and structure refinement for complexes **1** and **3**

	1	3
Empirical formula	C ₃₆ H ₃₀ BrCuN ₆ O ₃ S ₆	C ₃₆ H ₃₀ Br _{0.72} Cl _{0.29} CuN ₆ O ₆ S ₃
Formula weight	930.47	870.19
Temperature (K)	110.15	110.15
Wavelength (Å)	0.71073	0.71073
Crystal system	Triclinic	Triclinic
Space group	<i>P</i> -1	<i>P</i> -1
Unit cell dimensions		

a (Å)	10.105(3)	9.942(2)
b (Å)	11.067(3)	10.631(2)
c (Å)	19.715(5)	19.827(4)
α (°)	100.277(3)	100.087(2)
β (°)	97.167(3)	97.217(2)
γ (°)	112.992(3)	111.760(2)
Volume (Å ³)	1950.6(8)	1874.1(7)
Z	2	2
Density (calculated) Mg/m ³	1.584	1.542
Absorption coefficient (mm ⁻¹)	1.950	1.592
$F(000)$	944	886
Crystal size (mm ³)	0.485×0.244×0.068	0.336×0.245×0.099
Theta range for data collection (°)	2.064 to 27.458	1.067 to 27.479
Index ranges	-13≤ h ≤13, -14≤ k ≤14, -25≤ l ≤25	-12≤ h ≤12, -13≤ k ≤13, -25≤ l ≤25
Reflections collected	22623	21812
Independent reflections [R(int)]	8769	8455
Completeness to theta= 25.242°	99.6%	99.7 %
Absorption correction	Semi-empirical from equivalents	Semi-empirical from equivalents
Max. and min. transmission	0.7456 and 0.4769	0.7456 and 0.6002
Refinement method	Full-matrix least-	Full-matrix least-squares on

	squares on F^2	F^2
Data / restraints / parameters	8769/0/478	8455/768/613
Goodness-of-fit on F^2	1.032	1.026
Final R indices [$I > 2\sigma(I)$]	R1=0.0492, wR2=0.0985	R1 = 0.0423, wR2 = 0.0857
R indices (all data)	R1=0.0849, wR2=0.1125	R1 = 0.0653, wR2 = 0.0948
Largest diff. peak and hole ($e.\text{\AA}^{-3}$)	0.534 and -1.033	0.615 and -0.514

Table 2 Selected bond lengths (\AA) and angles ($^\circ$) of complexes **1** and **3**

	1	3
Br(1)–Cu(1)	2.4959(7)	2.470(4)
Cu(1)–S(1)	2.2709(12)	2.2694(9)
Cu(1)–S(3)	2.2720(11)	2.2969(9)
Cu(1)–S(5)/S(2)	2.3034(11)	2.2749(9)
S(1)–Cu(1)–Br(1)	110.41(4)	112.21(8)
S(1)–Cu(1)–S(3)	111.37(4)	107.02(3)
S(1)–Cu(1)–S(5)/S(2)	110.56(4)	110.07(3)
S(3)–Cu(1)–Br(1)	108.52(4)	107.04(10)
S(3)/S(2)–Cu(1)–S(5)/S(3)	108.15(4)	111.35(3)
S(5)/S(2)–Cu(1)–Br(1)	107.72(4)	109.12(9)
C(1)–S(1)–Cu(1)	109.10(14)	112.08(10)
C(13)/C(25)–S(3)–Cu(1)	112.31(14)	109.11(11)

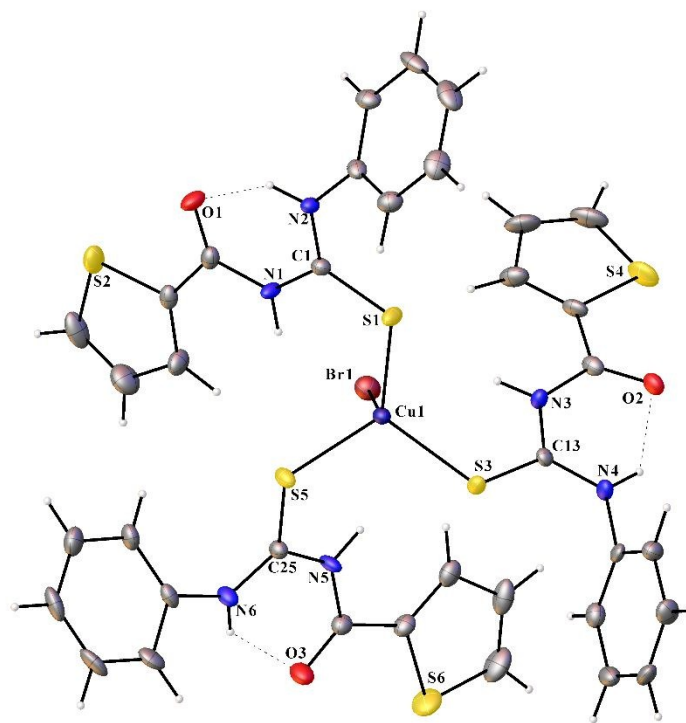


Fig. 2 Molecular structure of 1.

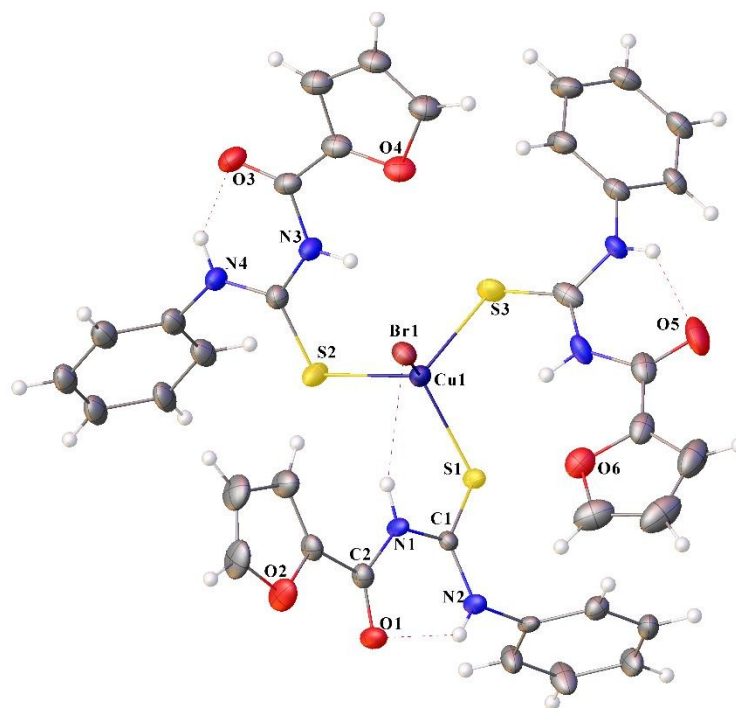


Fig. 3 Molecular structure of 3.

2.4. DNA interaction studies

2.4.1. Electronic spectroscopic studies

The binding mode of metal complexes with DNA can be effectively interpreted by electronic absorption spectroscopy.²⁷⁻²⁹ The electronic absorption spectra of Cu(I) complexes **1-4** exhibited a band around 293-297 nm which corresponded to intraligand transition. On titration of the complexes (1.0×10^{-5} M) with CT DNA, the absorption intensity decreased, resulting in hypochromism with a small red shift. The binding ability of complexes influences extent of shift and hypochromicity, and it normally correlates with the intercalative binding strength. The magnitude of hypochromism (**4**>**2**>**1**>**3**) reflected the DNA binding affinity of the complexes. (Figs. 4 and S11).

From the observed spectral changes, binding constant of the complexes with CT DNA (K_b) was obtained. The binding constant was calculated by plotting $[\text{DNA}]/(\epsilon_a - \epsilon_f)$ against $[\text{DNA}]$ according to the equation $[\text{DNA}]/(\epsilon_a - \epsilon_f) = [\text{DNA}]/(\epsilon_b - \epsilon_f) + 1/K_b (\epsilon_b - \epsilon_f)$ where $[\text{DNA}]$ is the concentration of DNA in base pairs, ϵ_a is the apparent extinction coefficient value found by calculating $A(\text{observed})/[\text{complex}]$, ϵ_f is the extinction coefficient for the free compound, and ϵ_b is the extinction coefficient for the compound in the fully bound form. Each set of data, when fitted into the above equation, gave a straight line with a slope of $1/(\epsilon_b - \epsilon_f)$ and an y-intercept of $1/K_b (\epsilon_b - \epsilon_f)$, and the value of K_b was determined from the ratio of slope to intercept (Fig. 5). The magnitudes of intrinsic binding constant (K_b) are given in Table 3. The observed values of K_b revealed that the Cu(I) complexes bound to DNA *via* intercalative mode.³⁰ The K_b values were found to be in the range of 9.5850×10^3 - 2.1046×10^4 M⁻¹. The enhanced binding ability of complexes **2** and **4** was due to the presence of planar naphthyl ring.

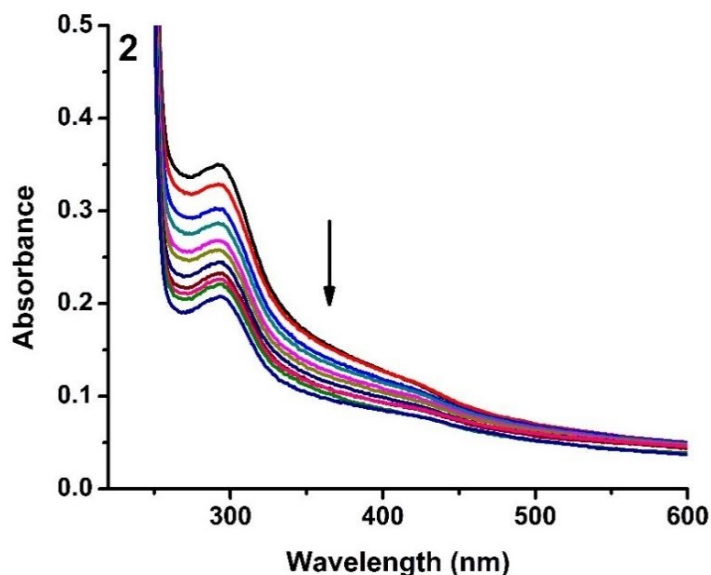


Fig. 4 Absorption spectra of complex 2 in Tris-HCl buffer upon addition of CT DNA. [Complex] = 1.0×10^{-5} M, [DNA] = 0-50 μ M. Arrow shows that the absorption intensities decrease upon increasing DNA concentration.

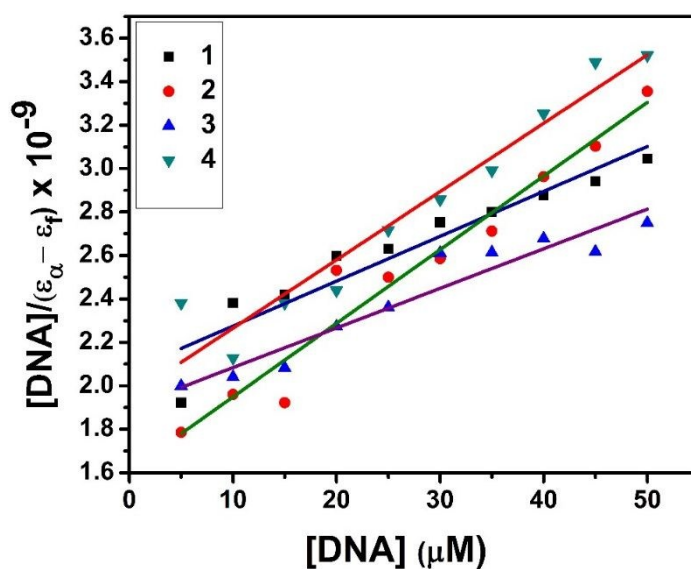
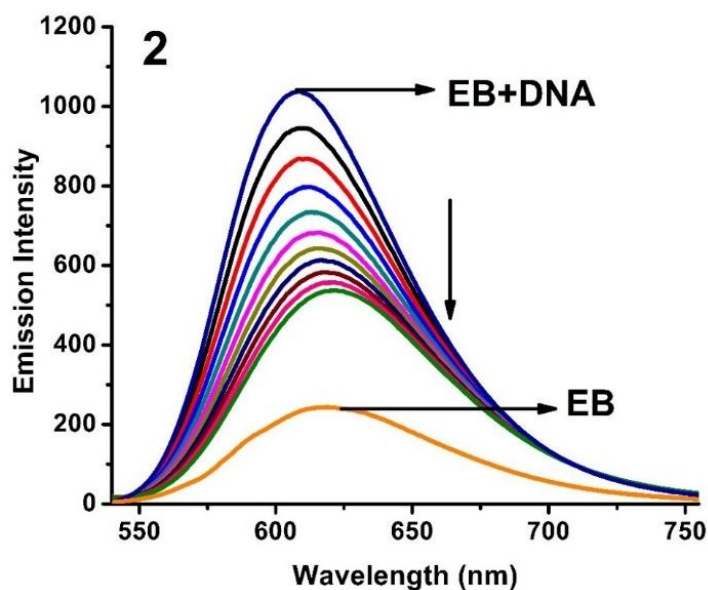


Fig. 5 Plots of $[DNA]/(\epsilon_a - \epsilon_f)$ versus $[DNA]$ for the titration of complexes with CT DNA.

2.4.2. Fluorescence spectroscopic studies

The complexes did not exhibit fluorescence property at room temperature in solution or in the presence of CT DNA. So binding of the complexes with DNA could not be directly predicted through the emission spectra. Hence, competitive binding study was done to confirm the mode of DNA binding with the complexes.³¹⁻³³ Ethidium bromide (EB) is a classical intercalator and

1
2
3 therefore it emits intense fluorescence in the presence of CT DNA. On titration of the complexes
4 with DNA bound EB, there was a quenching in the emission of DNA bound EB at 605 nm (Figs.
5 6 and S12). The quenching proved that the complexes replaced EB and bound more strongly with
6 DNA. The extent of quenching of CT DNA-EB reflects the extent of interaction with the added
7 molecule. Fluorescence quenching is explained by the Stern-Volmer equation³⁴ $F^0/F = 1 + K_q [Q]$
8 where F^0 and F are the fluorescence intensities in the absence and presence of complex
9 respectively, K_q is a linear Stern-Volmer quenching constant, and $[Q]$ is the concentration of
10 complex. The slope of the plot of F^0/F versus $[Q]$ gave K_q (Fig. 7). The apparent DNA binding
11 constant (K_{app}) values were calculated by using the equation $K_{EB} [EB] = K_{app} [complex]$, where
12 $[complex]$ is the complex concentration at 50% reduction in the fluorescence intensity of EB, K_{EB}
13 = $1.0 \times 10^7 \text{ M}^{-1}$ and $[EB] = 5 \mu\text{M}$. The quenching constant K_q and K_{app} values are listed in Table 3.
14 The observed binding constants are comparable with the previously reported copper(I)
15 complexes.²²



16
17
18
19
20
21
22
23
24
25
26
27
28
29
30
31
32
33
34
35
36
37
38
39
40
41
42
43
44
45
46
47 **Fig. 6** Fluorescence quenching curves of EB bound to DNA in the presence of **2**. $[DNA] = 5 \mu\text{M}$,
48 $[EB] = 5 \mu\text{M}$ and $[complex] = 0-50 \mu\text{M}$.
49
50
51
52
53
54
55
56
57
58
59
60

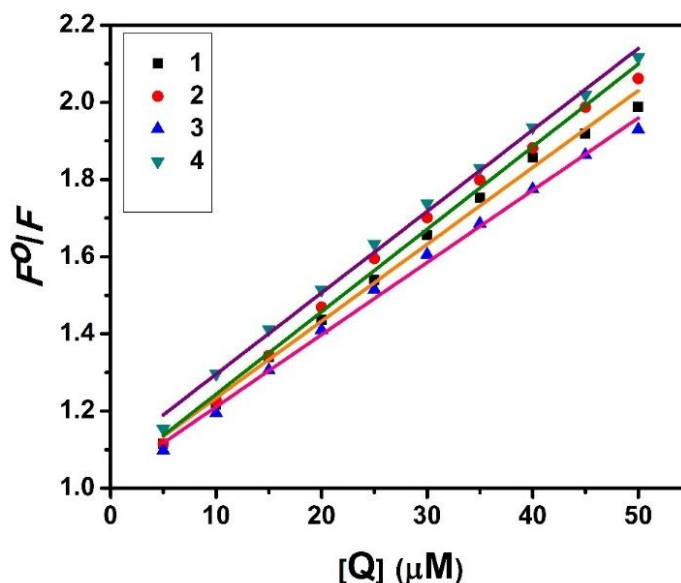


Fig. 7 Stern-Volmer plots of fluorescence titrations of the complexes with CT DNA.

Table 3 DNA binding constant (K_b), Stern-Volmer constant (K_q) and the apparent binding constant (K_{app}) for complexes 1-4

Complex	K_b (M^{-1})	K_q (M^{-1})	K_{app} (M^{-1})
1	9.98×10^3	1.87×10^4	9.35×10^5
2	2.10×10^4	2.13×10^4	1.06×10^6
3	9.58×10^3	1.78×10^4	8.94×10^5
4	1.67×10^4	2.11×10^4	1.05×10^6

2.5. Protein binding studies

2.5.1. Absorption and emission spectroscopic studies

The electronic absorption titration of BSA with the complexes (1-4) was carried out to validate the type of quenching process. On addition of the complexes to BSA, there was an increase in BSA absorption intensity at 280 nm without any red/blue shift. This clearly indicated a static type of interaction between the Cu(I) complexes and BSA.³⁵ The UV-Visible titration spectra are shown in Fig. 8.

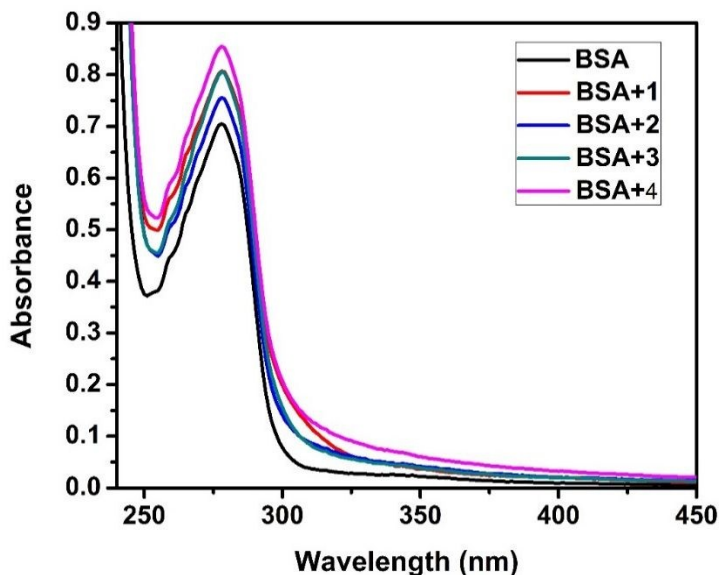


Fig. 8 The absorption spectra of BSA (10 μM) and BSA with 1-4 (4 μM).

Figure S13 shows the fluorescence emission spectra of BSA after the addition of complexes (1-4). On incremental addition of the complexes to the fixed quantity of BSA, there was a decrease in the fluorescence intensity of BSA at 345 nm. The percentage decrease in fluorescence intensity was 81.0, 69.2, 75.22 and 86.3 % for complexes 1-4 respectively, with hypsochromic shift of 1, 2 and 2 nm for complexes 1, 2 and 3 respectively. The observed spectral changes predicted that the complexes interacted hydrophobically with BSA.³⁶ The fluorescence quenching is described by the Stern-Volmer relation $F^0/F = 1 + K_q [Q]$ where F^0 and F demonstrate the fluorescence intensities in the absence and presence of quencher, respectively. K_q is a linear Stern-Volmer quenching constant, and $[Q]$ is the quencher concentration. The quenching constant (K_q) can be calculated using the plot of F^0/F versus $[Q]$ (Fig. S14). When small molecules bind independently to a set of equivalent site, on a macromolecule, the equilibrium between free and bound molecules is represented by the Scatchard equation^{37,38} $\log[(F^0-F)/F] = \log K_b + n \log [Q]$ where K_b is the binding constant of complex with BSA and n is the number of binding sites. From the plot of $\log[(F^0-F)/F]$ versus $\log [Q]$ (Fig. S15), the number of binding sites (n) and the binding constant (K_b) values have been calculated. The quenching constant (K_q), binding constant (K_b) and number of binding sites (n) for the interaction of the Cu(I) complexes with BSA are shown in Table 4. The binding, quenching constants correlates with the previously reported copper(I) complexes.²² In all the complexes, the number of binding sites is one. Results revealed that complexes 1 and 4 interacted strongly with BSA compared to 2 and 3.

Table 4 Protein binding constant (K_b), quenching constant (K_q) and number of binding sites (n) for complexes **1-4**

Complex	K_b (M^{-1})	K_q (M^{-1})	n
1	1.75×10^6	4.46×10^5	1.27
2	5.39×10^4	2.12×10^5	0.87
3	6.64×10^5	3.09×10^5	1.07
4	3.65×10^6	6.61×10^5	1.16

2.5.2. Synchronous fluorescence spectroscopic studies

Synchronous fluorescence spectroscopy provides information about the molecular microenvironment, particularly in the vicinity of the fluorophore functional groups.^{39,40} The fluorescence property of BSA is due to the presence of tyrosine, tryptophan and phenylalanine residues. The difference between the excitation and emission wavelengths ($\Delta\lambda$) reflects the nature of the chromophore. The large $\Delta\lambda$ value, such as 60 nm is characteristic of tryptophan residue, and small $\Delta\lambda$ value, such as 15 nm is characteristic of tyrosine. The synchronous fluorescence spectra of BSA with various concentrations of the Cu(I) complexes (**1-4**) were recorded at $\Delta\lambda = 15$ and 60 nm. The incremental addition of complexes decreased the fluorescence intensity of tyrosine residue at 300 nm in the magnitude of 86.4, 64.3, 70.5 and 87.3 % for complexes **1-4** respectively (Fig. S16). Similarly, the decrease observed in the intensity of tryptophan residue at 340 nm was 80.0, 66.5, 72.7 and 85.6 % for complexes **1-4** respectively (Fig. S17). The results showed that all the complexes affected the microenvironments of both tyrosine and tryptophan residues and the effect was more pronounced towards tyrosine than tryptophan.

2.6. Cytotoxic property of the compounds

The compounds (L1-L4, CuBr and **1-4**) were screened for their cytotoxic property against a panel of five human cancer (A549, HeLa S3, PANC-1, MIA PaCa2 and HeLa) and one normal (IMR90) cell lines. The graph of percentage of cell viability *versus* concentration is shown in Figs. 9, S18 and S19. The half minimum inhibitory concentration (IC_{50}) values calculated for the compounds are tabulated (Table 5). Complexes **1-4** showed promising cytotoxic activity against HeLa cancer cells. Interestingly complexes **1**, **2** and **3** exhibited excellent activity against HeLa cell line with IC_{50} value of 1.23, 0.47 and 1.84 μ M respectively, which are comparable with the previously reported copper(I) complexes.⁴¹ Besides, complexes **1**, **2** and **3** showed potent ability

to kill the MIA PaCa2 cells with IC_{50} value of 4.32, 4.96 and 3.01 μM respectively. Complexes **1** and **2** were active against PANC-1 cell line with IC_{50} value of 7.3 and 8.09 μM respectively. The present complexes also exhibited appreciable activity ($IC_{50} = 12.2 - 29 \mu\text{M}$) against A549 and HeLa S3 cell lines. The cytotoxic results of ligands ($> 100 \mu\text{M}$) against A549 and HeLa S3 cell lines clearly indicated that complexation played a key role in enhancing the activity. It is noteworthy to mention that the present complexes are more active than the well-known anticancer agents such as gemcitabine and cisplatin.⁴² There is hardly a correlation between DNA/protein binding results and cytotoxicity, which reveals that the enhanced cytotoxicity of complexes is not due to DNA/protein binding; there might be a different cytotoxic mechanism.^{22,43}

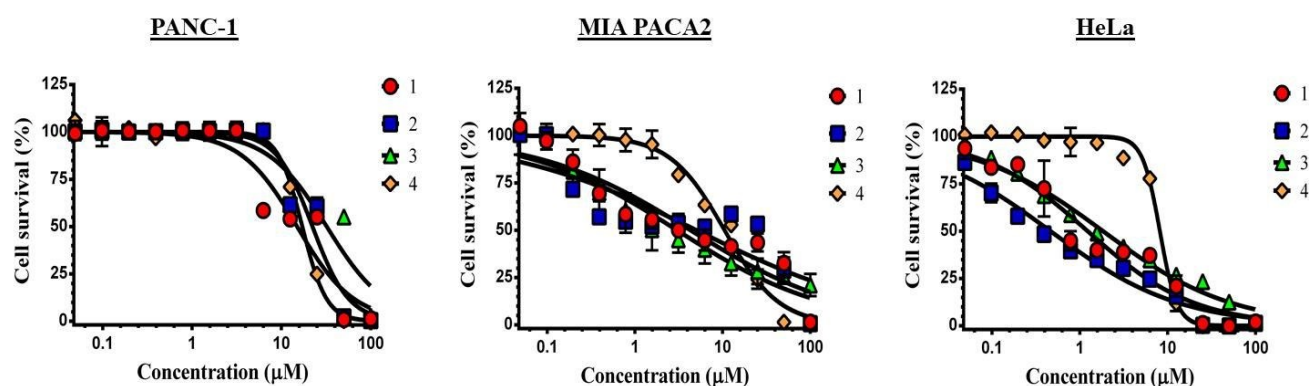


Fig. 9 Cytotoxic effects of complexes **1-4** against PANC-1, MIA PaCa2 and HeLa cells. The data were expressed in $SD \pm \text{mean}$ with three replications.

Table 5 IC_{50} values (μM) of the compounds against A549, HeLa S3, HeLa, PANC-1, MIA PaCa2 and IMR90 cells after 24 h.

Complex	A549	HeLa S3	HeLa	PANC-1	MIA PaCa2	IMR90
L1	>100	>100	NT	NT	NT	NT
L2	>100	>100	NT	NT	NT	NT
L3	>100	>100	NT	NT	NT	NT
L4	>100	>100	NT	NT	NT	NT
CuBr	>100	>100	NT	NT	NT	NT
1	17.7	12.6	1.23	7.3	4.32	26.3
2	18.1	12.2	0.47	8.09	4.96	10
3	25.9	21.9	1.84	14.34	3.01	52.5

4	29	13.4	8.14	14.23	12.32	31.1
Gemcitabine	-	-	-	>25	>25	-
Cisplatin ⁴⁴	18	-	22.4	15	-	-

NT-Not Tested

2.7. Acridine orange/ethidium bromide staining

Acridine orange/ethidium bromide staining was carried out to view the morphological changes associated with apoptotic cell death. Acridine orange (AO) is a dye that could stain nuclear DNA and RNA with an intact cell membrane, and ethidium bromide (EB) could only stain cells that had lost membrane integrity.⁴⁵ The morphological changes in the HeLa cancer cell line after treatment with 5 μ M concentration of **1** and **2** are shown in figure 10. The control cells exhibited normal green nucleus with intact membrane. The cells treated with complexes **1** and **2** displayed remarkable changes in the morphology such as irregularity in shape and membrane blebbing.

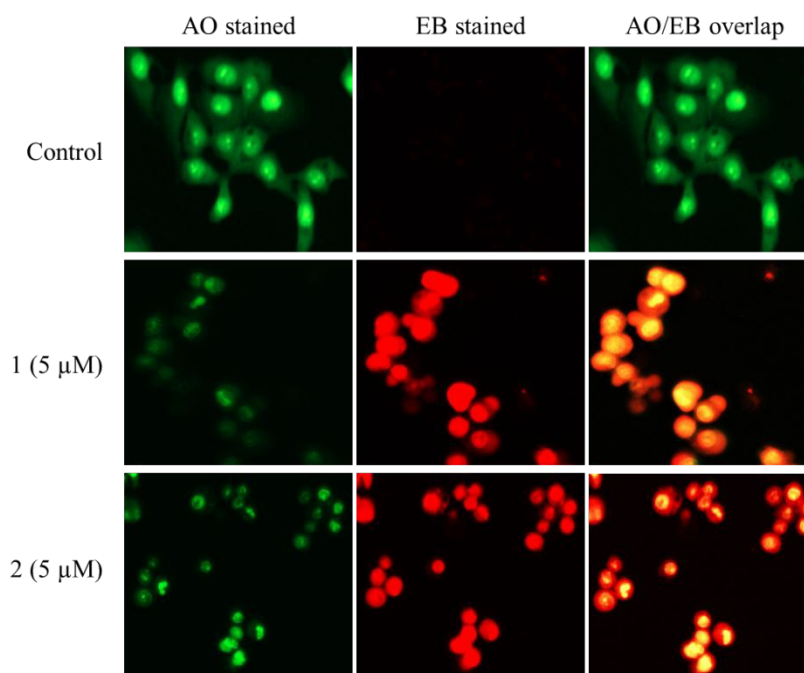


Fig. 10 Effect of **1** and **2** against HeLa cells. Images are taken under fluorescence microscope. AO indicates live cells and EB indicates dead cells.

The early apoptotic cells were characterized by greenish yellow colour with condensed chromatin whereas the late apoptotic cells were indicated by orange red nucleus with chromatin condensation and nuclear fragmentation. Staining studies confirmed that the complexes induced apoptosis in the cancer cell lines.

2.8. Colony formation studies

Colony formation study is a technique used to evaluate the effectiveness of a cell to proliferate effectively, which consequently retains its reproductive ability to form colonies. Complexes **1** and **2** were treated with HeLa cells to assess the colony formation ability (Fig. 11). The results confirmed that complex **1** showed complete inhibition of colony formation at 4 μM concentration. Complex **2** also inhibited 80% of colony formation at 4 μM concentration.

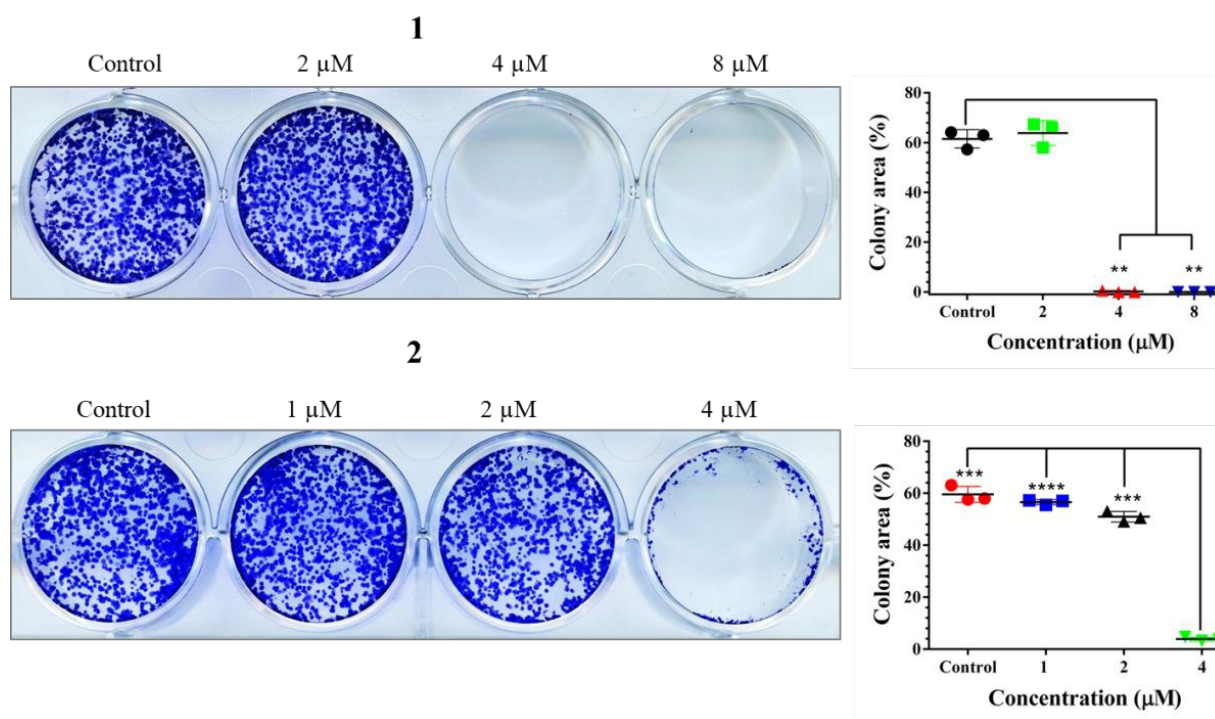


Fig. 11 Effects of **1** and **2** on colony formation studies. The data were obtained by using ImageJ software under colony area with three independent experiments. **** $p < 0.0001$, *** $P < 0.001$ and ** $P < 0.001$ ($n = 3$), significance was compared with treated and untreated groups.

3. Conclusion

A series of copper(I) complexes containing aroylthiourea ligands has been synthesized and characterized by analytical and spectroscopic techniques. The Cu(I) complexes adopt a tetrahedral geometry which was confirmed by crystallographic technique. The binding ability of the complexes with DNA/BSA was validated using spectroscopic techniques. *In vitro* cytotoxic assay revealed appreciable activity of the complexes against A549, HeLa S3, HeLa, PANC-1 and MIA PaCa2 cancer cell lines. Complex **2** showed phenomenal activity with least IC_{50} value (0.47 μM)

against HeLa cell line. Further the most active complexes were subjected to staining and colony formation experiments. The staining studies proved the apoptosis mechanism of cell death and colony formation experiments demonstrated the ability of the complexes to inhibit the colony formation effectively. On conclusion, the Cu(I) complexes interacted with DNA/BSA appreciably, exhibited excellent cytotoxicity against tested cancer cell lines. Further investigation may lead to the development of potential anticancer agent.

4. Experimental section

4.1. Materials and methods

All the chemicals were purchased from Sigma Aldrich / Merck and used as received. Solvents were purified according to standard procedures. The melting points were determined on Lab India instrument and are uncorrected. The elemental analyses were performed using a Vario EL-III CHNS analyzer. FT-IR spectra were obtained as KBr pellets using a Nicolet-iS5 spectrophotometer. UV-Visible spectra were recorded using a Shimadzu-260 spectrophotometer. Emission spectra were measured on a Jasco V-630 spectrophotometer using 5 % DMF in buffer as a solvent. NMR spectra were recorded in CDCl₃ by using TMS as an internal standard on a Bruker 400/500 MHz spectrometer. A549, HeLa S3, HeLa, PANC-1, MIA PaCa2 and IMR90 cells were purchased from the Riken BRC, Japan.

4.2. Synthesis of the ligands

The ligands were synthesized by following the reported procedure. L1, L2 and L3 were already reported.²³ L4 was synthesized from the reaction between furoyl chloride, potassium thiocyanate and 1-naphthylamine.

4.2.1. N-(naphthalen-1-ylcarbamothioyl)furan-2-carboxamide (L4)

Furoyl chloride (1.4057 g, 10 mmol) and 1-naphthylamine (1.4319 g, 10 mmol) were used. Yield: 80 %. White solid. M.p.: 195 °C. Anal. calcd. for C₁₆H₁₂N₂O₂S: C, 64.85; H, 4.08; N, 9.45; S, 10.82. Found: C, 64.13; H, 3.98; N, 9.28; S, 10.18. UV-Vis (CHCl₃): λ_{max}, nm (ε, dm³mol⁻¹cm⁻¹) 269 (7533), 294 (9933). FT-IR (KBr, cm⁻¹): 3657 (m; ν(amide N-H)), 3218 (s; ν(thiourea N-H)), 1663 (s; ν(C=O)), 1270 (s; ν(C=S)). ¹H NMR (500 MHz, CDCl₃) δ, ppm 12.47 (s, 1H), 9.39 (s, 1H), 8.01 (dd, *J* = 13.4, 7.9 Hz, 2H), 7.90 (d, *J* = 7.5 Hz, 1H), 7.84 (d, *J* = 8.3 Hz, 1H), 7.62 (d, *J* = 0.9 Hz, 1H), 7.60-7.50 (m, 3H), 7.42 (d, *J* = 3.2 Hz, 1H), 6.64 (dd, *J* = 3.6, 1.7 Hz, 1H). ¹³C

NMR (126 MHz, CDCl₃) δ , ppm 179.6, 157.0, 146.6, 145.0, 134.2, 133.5, 128.6, 128.5, 128.0, 127.0, 126.4, 125.2, 123.9, 121.6, 119.1, 113.5.

4.3. Synthesis of the copper(I) complexes

Copper(I) bromide (28.6 mg, 0.2 mmol) dissolved in acetonitrile (5 mL) was added to the ligand (0.6 mmol) in acetonitrile (10 mL). Then 0.5 % HCl (2 mL) was added, which turned the reaction mixture to green colour. The resultant solution was stirred at room temperature for 24 h. The pale yellow solid was filtered off, washed with hexane and dried in *vacuum*. The solid was recrystallized in chloroform/methanol mixture (1:9) to get suitable crystals for X-ray diffraction.

4.3.1. [CuBr(L1)₃] (1)

L1 (157.4 mg, 0.6 mmol) was used. Yield: 80 %. Pale yellow solid. M.p.: 210 °C. Anal. calcd. for C₃₆H₃₀BrCuN₆O₃S₆: C, 46.47; H, 3.25; N, 9.03; S, 20.68. Found: C, 46.13; H, 3.06; N, 9.17; S, 20.18. UV-Vis (DMF): λ_{\max} , nm (ϵ , dm³mol⁻¹cm⁻¹) 267 (50600), 293 (58900). FT-IR (KBr, cm⁻¹): 3265 (m; ν (amide N-H)), 3129 (s; ν (thiourea N-H)), 1663 (s; ν (C=O)), 1155 (s; ν (C=S)). ¹H NMR (400 MHz, CDCl₃): δ , ppm 12.61 (s, 1H), 10.56 (s, 1H), 8.54 (dd, J = 3.9, 0.9 Hz, 1H), 7.72 (dd, J = 5.0, 0.9 Hz, 1H), 7.46 (d, J = 7.9 Hz, 2H), 7.37 (t, J = 7.7 Hz, 2H), 7.29 (d, J = 7.4 Hz, 1H), 7.17 (dd, J = 4.9, 4.0 Hz, 1H). ¹³C NMR (101 MHz, CDCl₃): δ , ppm 178.3, 162.8, 136.7, 135.8, 134.9, 133.4, 129.0, 128.7, 127.6, 125.1.

4.3.2. [CuBr(L2)₃] (2)

L2 (187.4 mg, 0.6 mmol) was used. Yield: 78 %. Pale yellow solid. M.p.: 231 °C. Anal. calcd. for C₄₈H₃₆BrCuN₆O₃S₆: C, 53.35; H, 3.36; N, 7.78; S, 17.80. Found: C, 53.63; H, 3.06; N, 7.67; S, 17.18. UV-Vis (DMF): λ_{\max} , nm (ϵ , dm³mol⁻¹cm⁻¹) 266 (23000), 297 (30300). FT-IR (KBr, cm⁻¹): 3434 (m; ν (amide N-H)), 3213 (s; ν (thiourea N-H)), 1656 (s; ν (C=O)), 1211 (s; ν (C=S)). ¹H NMR (400 MHz, CDCl₃): δ , ppm 12.87 (s, 1H), 11.10 (s, 1H), 8.77 (d, J = 3.7 Hz, 1H), 7.88 (dd, J = 8.8, 3.6 Hz, 2H), 7.85 (d, J = 8.2 Hz, 1H), 7.78 (d, J = 4.9 Hz, 1H), 7.65 (d, J = 7.3 Hz, 1H), 7.55-7.50 (m, 2H), 7.50-7.45 (m, 1H), 7.24 (d, J = 5.0 Hz, 1H). ¹³C NMR (101 MHz, CDCl₃): δ , ppm 180.5, 163.7, 135.3, 134.2, 128.8, 128.5, 127.3, 126.6, 125.1, 124.8, 121.8.

4.3.3. [CuBr(L3)₃] (3)

L3 (147.7 mg, 0.5 mmol) was used. Yield: 85 %. Pale yellow solid. Anal. calcd. for C₃₆H₃₀BrCuN₆O₆S₃: C, 49.01; H, 3.43; N, 9.53; S, 10.90. Found: C, 48.63; H, 3.56; N, 9.67; S, 10.18. M.p.: 179 °C. UV-Vis (DMF): λ_{\max} , nm (ϵ , dm³mol⁻¹cm⁻¹) 270 (51200), 293 (46300). FT-

IR (KBr, cm^{-1}): 3260 (m; $\nu(\text{amide N-H})$), 3215 (s; $\nu(\text{thiourea N-H})$), 1675 (s; $\nu(\text{C=O})$), 1247 (s; $\nu(\text{C=S})$). ^1H NMR (500 MHz, CDCl_3): δ , ppm 12.53 (s, 1H), 10.45 (s, 1H), 7.86 (d, $J = 2.9$ Hz, 1H), 7.67 (d, $J = 7.2$ Hz, 1H), 7.51 (d, $J = 7.7$ Hz, 2H), 7.39 (t, $J = 7.5$ Hz, 2H), 7.30 (t, $J = 7.3$ Hz, 1H), 6.61 (d, $J = 1.6$ Hz, 1H). ^{13}C NMR (126 MHz, CDCl_3): δ , ppm 178.4, 158.2, 147.6, 144.5, 136.7, 129.0, 127.65, 125.1, 120.1, 113.0.

4.3.4. $[\text{CuBr}(\text{L4})_3]$ (4)

L4 (177.8 mg, 0.6 mmol) was used. Yield: 73 %. Pale yellow solid. Anal. calcd. for $\text{C}_{48}\text{H}_{36}\text{BrCuN}_6\text{O}_6\text{S}_3$: C, 55.84; H, 3.51; N, 8.14; S, 9.32. Found: C, 55.63; H, 3.16; N, 8.67; S, 9.18. M.p.: 216 $^\circ\text{C}$. UV-Vis (DMF): λ_{max} , nm (ϵ , $\text{dm}^3\text{mol}^{-1}\text{cm}^{-1}$) 274 (54400), 294 (57900). FT-IR (KBr, cm^{-1}): 3447 (m; $\nu(\text{amide N-H})$), 3224 (s; $\nu(\text{thiourea N-H})$), 1679 (s; $\nu(\text{C=O})$), 1249 (s; $\nu(\text{C=S})$). ^1H NMR (500 MHz, DMSO-d_6): δ , ppm 12.51 (s, 1H), 11.49 (s, 1H), 8.19-8.16 (m, 1H), 8.09 (d, $J = 7$ Hz, 1H), 8.02 (d, $J = 4$ Hz, 3H), 7.82 (d, $J = 6$ Hz, 1H), 7.66 (d, $J = 6$ Hz, 3H), 6.88-6.86 (m, 1H). ^{13}C NMR (126 MHz, DMSO-d_6): δ , ppm 180.8, 158.1, 149.0, 145.2, 134.5, 134.2, 129.1, 128.8, 128.1, 127.2, 126.8, 125.9, 123.2, 122.7, 119.5, 113.2.

4.4. X-ray crystallography

A BRUKER APEX 2 X-ray (three-circle) diffractometer was employed for crystal screening, unit cell determination, and data collection. Integrated intensity information for each reflection was obtained by reduction of data frames with APEX2.⁴⁶ SADABS was employed to correct the data for absorption effects.⁴⁷ A solution was obtained readily by using SHELXT (XT).^{48,49} Hydrogen atoms were placed in idealized positions and were set riding on the respective parent atoms. All the non-hydrogen atoms were refined with anisotropic thermal parameters. Absence of additional symmetry and / or voids was confirmed by using PLATON. Olex2 was employed for final data presentation and structure plots.⁵⁰

4.5. DNA binding experiments

For absorption spectral studies, CT-DNA was dissolved in 50 mM NaCl/5 mM Tris-HCl (pH 7.2) solution. The DNA solution displayed a UV absorbance ratio (A_{260}/A_{280}) of 1.9:1, indicating that the DNA was sufficiently in protein free form. Further, dilution of DNA solution was made in such a way that its maximum absorbance should be 260 nm with the absorption coefficient value of $6600 \text{ cm}^{-1}\text{M}^{-1}$ per nucleotide.^{51,52} The synthesized complexes were dissolved using 5 % DMF/Tris-HCl/NaCl buffer.

There was an urge for the ethidium bromide (EB) displacement study due the non-emissive property of the copper(I) complexes. The competitive binding study has been carried out using fluorescence spectroscopic technique to find out the efficacy of the complexes to displace EB from DNA-EB complex. The experiment was carried out by fixing the excitation wavelength at 510 nm and the spectra were recorded from 520 to 800 nm. In this experiment, DNA-EB concentration was fixed and the changes in the emission intensity were measured by titrating with the complexes in aliquots of 5 μ M.⁵³

4.6. Protein binding experiments

Binding efficacy of the Cu(I) complexes with Bovine Serum albumin (BSA) was analyzed using fluorescence spectra recorded at a fixed excitation wavelength corresponding to BSA (280 nm) and monitoring the emission at 345 nm. The excitation and emission slit widths and scan rates were constantly maintained for all the experiments. The stock solution of BSA was prepared using 50 mM phosphate buffer (pH = 7.2) and stored in the dark at 4 °C for further use. The stock solutions of complexes were prepared using DMF-phosphate buffer (5:95) and were further diluted to the required concentration using phosphate buffer. 2.5 mL of BSA solution was titrated by successive additions of 10^{-6} M stock solution of the complexes using a micropipette. Synchronous spectra were also recorded using the same concentration of BSA and complexes as mentioned above at two different $\Delta\lambda$ (difference between the excitation and emission wavelengths of BSA) values of 15 and 60 nm.

4.7. *In vitro* cytotoxicity evaluation by MTT assay

Cytotoxicity of the compounds was tested against human lung (A549 and IMR90-normal), human cervical (HeLa S3 and HeLa), human pancreatic epitheloid (PANC-1) and human caucasian pancreatic (MIA PaCa2) cell lines (2×10^4 /well). Standard 3-[4,5-dimethylthiazol-2-yl]-2,5-diphenyltetrazolium bromide (MTT) assay was used to evaluate the cell viability.⁵⁴⁻⁵⁷ The detailed experimental procedure is provided in the supporting information.

4.8. Fluorescence images

HeLa cells were seeded in 30 mm plates, treated with complexes **1** and **2** and incubated for 24 h. After treatment, cells were stained with AO/EB (acridine orange/ethidium bromide) for 15 minutes. The images were captured under EVOS (20x) microscope.

4.9. Colony formation studies

1×10^3 HeLa cells/well were cultured in 12 well plates and treated with different concentrations of **1** (2, 4 and 8 μM) and **2** (1, 2 and 4 μM) for 24 h. After 24 h treatment, cells were washed twice with PBS (phosphate buffer saline) and incubated with fresh DMEM (Dulbecco's Modified Eagle Medium) for 10 days. The cells were washed twice with distilled H_2O and stained with crystal violet for 10 min. After incubation, cells were washed with distilled H_2O and dried. The data were obtained by ImageJ under colony area.⁵⁸

4.10. Data analysis

Data were analyzed ($\text{SD} \pm \text{mean}$) with three independent experiments using Graphpad Prism 6. Significance was calculated by Tukey's multiple comparisons test ($p < 0.05$).

Acknowledgement

K. J. thanks the Department of Science and Technology, Ministry of Science and Technology, Government of India for doctoral fellowship under DST-INSPIRE programme. J. H. thanks the University Grants Commission for the fellowship (F1-17.1/2012-13/RGNF-2012-13-ST-AND-18716). R. K. gratefully acknowledges DST for the financial support. Authors also thank Prof. Toshiyuki Kaji and Dr. Eiko Yoshida, Faculty of Pharmaceutical Sciences, Tokyo University of Science, Japan for providing cell lines for carrying out the anticancer studies.

References

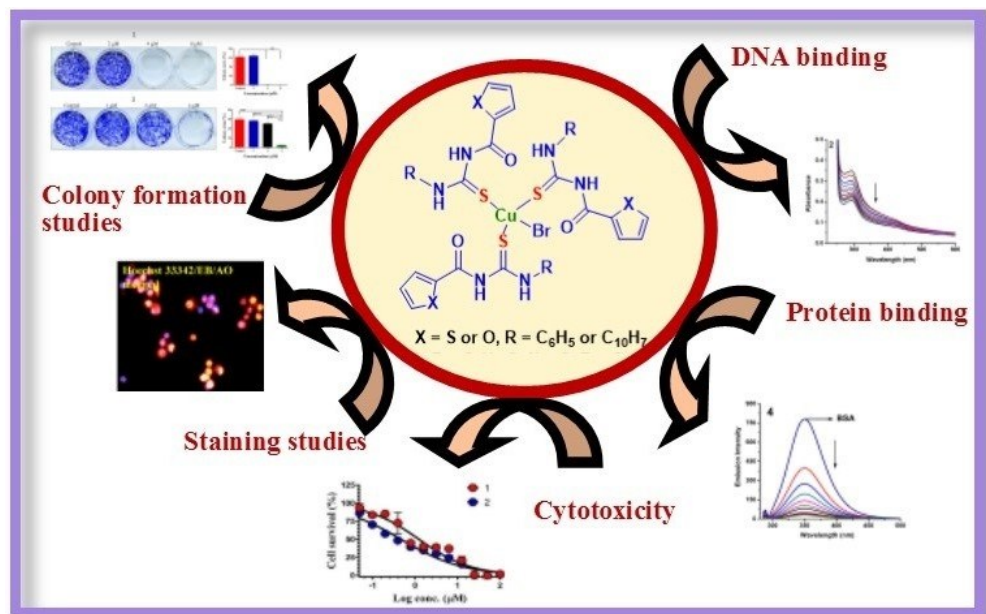
1. H. B. Kraatz, N. M. Nolte, Concepts and Models in Bioinorganic Chemistry; Wiley-VCH: Weinheim, Germany, 2006.
2. S. J. Lippard, J. M. Berg, Principles of Bioinorganic Chemistry; University Science Books: Mill Valley, CA, 1994.
3. J. J. R. Frausto da Silva, R. J. P. Williams, The biological chemistry of the elements; Clarendon: Oxford, U. K., 1991.
4. S. K. Hadjikakou, C. D. Antoniadis, P. Aslanidis, P. J. Cox and A. C. Tsipis, *Eur. J. Inorg. Chem.*, 2005, 1442-1452.
5. C. Marzano, M. Pellei, S. Alidori, A. Brossa, G. G. Lobbia, F. Tisato and C. Santini, *J. Inorg. Biochem.*, 2006, **100**, 299-304.
6. M. Porchia, F. Benetollo, F. Refosco, F. Tisato, C. Marzano and V. Gandin, *J. Inorg. Biochem.*, 2009, **103**, 1644-1651.

7. P. Aslanidis, P. J. Cox, P. Karagiannidis, S. K. Hadjikakou and C. D. Antoniadis, *Eur. J. Inorg. Chem.*, 2002, 2216-2222.
8. P. Karagiannidis, S. K. Hadjikakou, P. Aslanidis and A. Huntas, *Inorg. Chim. Acta*, 1990, **178**, 27-34.
9. S. K. Hadjikakou, P. Aslanidis, P. D. Akrivos, P. Karagiannidis, B. Kojic-Prodic and M. Luic, *Inorg. Chim. Acta*, 1992, **197**, 31-38.
10. P. Aslanidis, S. K. Hadjikakou, P. Karagiannidis, B. Kojic-Prodic and M. Luic, *Polyhedron*, 1994, **12**, 3119-3125.
11. P. D. Akrivos, S. K. Hadjikakou, P. Karagiannidis, D. Mentzafos and A. Terzis, *Inorg. Chim. Acta*, 1993, **206**, 163-168.
12. S. K. Hadjikakou, P. D. Akrivos, P. Karagiannidis, D. Mentzafos and A. Terzis, *Inorg. Chim. Acta*, 1993, **210**, 27-31.
13. Y. F. Yuan, J. T. Wang, M. C. Gimeno, A. Laguna and P. G. Jones, *Inorg. Chim. Acta*, 2001, **324**, 309-317.
14. Y. M. Zhang, T. B. Wei, L. Xian and L. M. Gao, *Phosphorus, Sulfur Silicon Relat. Elem.*, 2004, **179**, 2007-2013.
15. W. Q. Zhou, B. L. Li, L. M. Zhu, J. G. Ding, Z. Yong, L. Lu and X. J. Yang, *J. Mol. Struct.*, 2004, **690**, 145-150.
16. T. K. Venkatachalam, C. Mao and F. M. Uckun, *Bioorg. Med. Chem.*, 2004, **12**, 4275-4284.
17. C.W. Sun, H. Huang, M. Feng, X. L. Shi, X. D. Zhang and P. A. Zhou. *Bioorg. Med. Chem. Lett.*, 2006, **16**, 162-164.
18. N. Selvakumaran, S. W. Ng, E. R. T. Tiekink and R. Karvembu, *Inorg. Chim. Acta*, 2011, **376**, 278-284.
19. N. Selvakumaran, A. Pratheepkumar, S. W. Ng, E. R. T. Tiekink and R. Karvembu, *Inorg. Chim. Acta*, 2013, **404**, 82-87.
20. N. Selvakumaran, N. S. P. Bhuvanesh, A. Endo and R. Karvembu, *Polyhedron*, 2014, **75**, 95-109.
21. N. Selvakumaran, N. S. P. Bhuvanesh, P. M. Sivakumar and R. Karvembu, *Dalton Trans.*, 2014, **43**, 16395-16410.
22. N. Selvakumaran, L. Sandhiya, N. S. P. Bhuvanesh, K. Senthilkumar and R. Karvembu, *New J. Chem.* 2016, **40**, 5401-5413.

23. K. Jeyalakshmi, J. Haribabu, N. S. P. Bhuvanesh and R. Karvembu, *Dalton Trans.*, 2016, **45**, 12518-12523.
24. K. Jeyalakshmi, J. Haribabu, C. Balachandran, N. S. P. Bhuvanesh, N. Emi and R. Karvembu, *New J. Chem.*, 2017, **41**, 2672-2686.
25. H. O. Kolinowski, S. Berger, S. Brown, ¹³C NMR Spectroscopy, Thieme-Verlag, Stuttgart, Germany, 1984.
26. R. L. Girling and E. L. Amma, *Inorg. Chem.*, 1971, **10**, 335-340.
27. J. K. Barton and A. L. Rapheal, *J. Am. Chem. Soc.*, 1984, **106**, 2172-2176.
28. T. M. Kelly, A. B. Tossi, D. J. McConnell and T. C. Streckas, *Nucleic Acids Res.*, 1985, **13**, 6017-6034.
29. S. A. Tysoe, R. J. Morgan, A. D. Baker and T. C. Streckas, *J. Phys. Chem.*, 1993, **97**, 1707-1711.
30. J. S. Guerrero, P. C. Sanchez, E. R. Perez, F. V. Garcia, M. E. B. Gomez and L. R. Azuara, *Toxicology in Vitro*, 2011, **25**, 1376-1384.
31. N. Chitrapriya, T. S. Kamatchi, M. Zeller, H. Lee and K. Natarajan, *Spectrochim. Acta Part A*, 2011, **81**, 128-134.
32. J. R. Lakowicz and G. Webber, *Biochemistry*, 1973, **12**, 4161-4170.
33. B. C. Baguley and M. Lebre, *Biochemistry*, 1984, **23**, 937-943.
34. K. S. Ghosh, B. K. Sahoo, D. Jana and S. Dasgupta, *J. Inorg. Biochem.* 2008, **102**, 1711-1718.
35. P. L. Gentili, F. Ortica and G. Favaro, *J. Phys. Chem. B*, 2008, **112**, 16793-16801.
36. (a) E. Jayanthi, M. Anusuya, N. S. P. Bhuvanesh, K. A. Khalil and N. Dharmaraj, *J. Coord. Chem.*, 2015, **68 (20)** 3551-3565; (b) J. Haribabu, K. Jeyalakshmi, Y. Arun, N.S.P. Bhuvanesh, P.T. Perumal and R. Karvembu, *J. Biol. Inorg. Chem.*, 2017, **22**, 461-480.
37. M. Pait, B. Kundu, S. C. Kundu and D. Ray, *Inorg. Chim. Acta*, 2014, **418**, 30-41.
38. T. Bayraktutan and Y. Ongane, *Dyes and Pigments*, 2017, **142**, 62-68.
39. J. B. F. Lloyd, *Nature Phys. Sci.*, 1971, **231**, 64-65.
40. J. B. F. Lloyd, *J. Forensic Sci. Soc.*, 1971, **11**, 83-94.
41. D. S-. Gil, L. Ortego, R. P. Herrera, I. Marzoc and M. C. Gimeno, *Dalton Trans.*, 2017, **46**, 13745-13755.
42. S. Tardito, C. Isella, E. Medico, L. Marchio, E. Bevilacqua, M. Hatzoglou, O. Bussolati and R. F-. Gazzola, *J. Biol. Chem.*, 2009, **284**, 24306-24319.

- 1
2
3 43. N. J. Sanghamitra, P. Phatak, S. Das, A. G. Samuelson and K. Somasundaram, *J. Med. Chem.*,
4 2005, **48**, 977-985.
5
6 44. S. Aydin, M. Becit, A. Basaran and N. Basaran, *Toxicol. Lett.*, 2016, **258S**, S62–S324.
7
8 45. S. Ramakrishnan, D. Shakthipriya, E. Suresh, V. S. Periasamy, M. A. Akbarsha and
9 M. Palaniandavar, *Inorg. Chem.*, 2011, **50**, 6458-6471.
10
11 46. APEX2 “Program for Data Collection and Integration on Area Detectors”, Bruker AXS Inc.,
12 5465 East Cheryl Parkway, Madison, WI 53711-5373 USA.
13
14 47. G. M. Sheldrick, SADABS (version 2014/5): Program for Absorption Correction for Data from
15 Area Detector Frames, University of Gottingen.
16
17 48. G. M. Sheldrick, *Acta Cryst.*, 2008, **A64**, 112-122.
18
19 49. G. M. Sheldrick, *Acta Cryst.*, 2015, **A71**, 3-8.
20
21 50. O. V. Dolomanov, L. J. Bourhis, R. J. Gildea, J. A. K. Howard and H. Puschmann, *J. Appl.*
22 *Cryst.*, 2009, **42**, 339-341.
23
24 51. J. A. Simpson, K. H. Cheeseman, S. E. Smith and R. T. Dean, *Biochem. J.*, 1988, **54**, 519-523.
25
26 52. J. Haribabu, K. Jeyalakshmi, Y. Arun, N. S. P. Bhuvanesh, P. T. Perumal and R. Karvembu,
27 *RSC Adv.*, 2015, **5**, 46031-46049.
28
29 53. (a) W. D. Wilson, L. Ratmeyer, M. Zhao, L. Strekowski and D. Boykin, *Biochemistry*, 1993,
30 **32**, 4098-4104; (b) J. Haribabu, G. Sabapathi, M. Muthu Tamizh, C. Balachandran, N. S. P.
31 Bhuvanesh, P. Venuvanalingam and R. Karvembu, *Organometallics*, 2018, **37**, 1242-1257.
32
33 54. C. Balachandran, J. Haribabu, K. Jeyalakshmi, N. S. P. Bhuvanesh, R. Karvembu, N. Emi and
34 S. Awale, *J. Inorg. Biochem.*, 2018, **182**, 208-221.
35
36 55. C. Balachandran, Y. Arun, B. Sangeetha, V. Duraipandiyani, S. Awale, N. Emi, S. Ignacimuthu
37 and P. T. Perumal, *Biomed. Pharmacother.*, 2017, **93**, 796-806;
38
39 56. (a) C. Balachandran, N. Emi, Y. Arun, N. Yamamoto, V. Duraipandiyani, Y. Inaguma, A.
40 Okamoto, S. Ignacimuthu, N. A. Al-Dhabi and P. T. Perumal, *Chem. Biol. Interact.*, 2016, **249**, 23-
41 35; (b) J. Haribabu, M. Muthu Tamizh, C. Balachandran, Y. Arun, N. S. P. Bhuvanesh, A. Endo
42 and R. Karvembu, *New J. Chem.*, 2018, **42**, 10818-10832.
43
44 57. C. Balachandran, N. Emi, Y. Arun, Y. Yamamoto, B. Ahilan, B. Sangeetha, V. Duraipandiyani,
45 Y. Inaguma, A. Okamoto, S. Ignacimuthu, N.A. Al- Dhabi and P. T. Perumal, *Chem. Biol. Interact.*,
46 2015, **242**, 81-90.
47
48
49
50
51
52
53
54
55
56
57
58
59
60

1
2
3 58. C. Balachandran, K. C. Rao, Y. Arun, N. Emi, N. Yamamoto, Y. Inaguma, A. Okamoto and
4 P. T. Perumal, *RSC Adv.*, 2016, **6**, 96946-96962.
5
6
7
8
9
10
11
12
13
14
15
16
17
18
19
20
21
22
23
24
25
26
27
28
29
30
31
32
33
34
35
36
37
38
39
40
41
42
43
44
45
46
47
48
49
50
51
52
53
54
55
56
57
58
59
60



Cu(I) complexes bearing aroylthiourea ligands were synthesized and their biological properties were evaluated.

64x39mm (300 x 300 DPI)